Tailoring Photoisomerization Pathways in Donor-Acceptor Stenhouse Adducts

Lerch, Michael M.; Medved, Miroslav; Lapini, Andrea; Laurent, Adele D.; Iagatti, Alessandro; Bussotti, Laura; Szymanski, Wiktor; Buma, Wybren Jan; Foggi, Paolo; Di Donato, Mariangela

Published in:
The Journal of Physical Chemistry. A: Molecules, Spectroscopy, Kinetics, Environment, & General Theory

DOI:
10.1021/acs.jpca.7b10255

Publication date:
2018

THE JOURNAL OF PHYSICAL CHEMISTRY A

Article

Cite This: J. Phys. Chem. A 2018, 122, 955−964

pubs.acs.org/JPCA

Tailoring Photoisomerization Pathways in Donor−Acceptor Stenhouse Adducts: The Role of the Hydroxy Group

Published as part of The Journal of Physical Chemistry virtual special issue ?Time-Resolved Vibrational Spectroscopy?.

Michael M. Lerch,[†] Miroslav Medveď,[∇,○] Andrea Lapini,[§,⊥] Adèle D. Laurent,[◆] Alessandro Iagatti,[§,∥] Laura Bussotti,[§] Wiktor Szymański,[‡,†] Wybren Jan Buma,[¶] Paolo Foggi,[§,∥,#] Mariangela Di Donato,[*,§,∥] and Ben L. Feringa[*,†]

[†]Centre for Systems Chemistry, Stratingh Institute for Chemistry, University of Groningen, Nijenborgh 4, 9747 AG Groningen, The Netherlands

[‡]Department of Radiology, University of Groningen, University Medical Center Groningen, Hanzeplein 1, 9713 GZ Groningen, The Netherlands

[§]LENS (European Laboratory for Non Linear Spectroscopy), via N. Carrara 1, 50019 Sesto Fiorentino, Italy

[∥]INO (Istituto Nazionale di Ottica), Largo Fermi 6, 50125 Firenze, Italy

[⊥]Dipartimento di Chimica "Ugo Schiff", Università di Firenze, via della Lastruccia 13, 50019 Sesto Fiorentino, Italy

[#]Dipartimento di Chimica, Università di Perugia, via Elce di Sotto 8, 06100 Perugia, Italy

[∇]Regional Centre of Advanced Technologies and Materials, Department of Physical Chemistry, Faculty of Science, Palacký University in Olomouc, 17. listopadu 1192/12, CZ-771 46 Olomouc, Czech Republic

[○]Department of Chemistry, Faculty of Natural Sciences, Matej Bel University, Tajovského 40, SK-97400 Banská Bystrica, Slovak Republic

[◆]CEISAM, UMR CNRS 6230, BP 92208, 2 Rue de la Houssinière, 44322 Nantes, Cedex 3, France

[¶]Van't Hoff Institute for Molecular Sciences, University of Amsterdam, Science Park 904, 1098 XH Amsterdam, The Netherlands

Supporting Information

ABSTRACT: Donor−acceptor Stenhouse adducts (DASAs) are a rapidly emerging class of visible light-activatable negative photochromes. They are closely related to (mero)cyanine dyes with the sole difference being a hydroxy group in the polyene chain. The presence or absence of the hydroxy group has far-reaching consequences for the photochemistry of the compound: cyanine dyes are widely used as fluorescent probes, whereas DASAs hold great promise for visible light-triggered photoswitching. Here we analyze the photophysical properties of a DASA lacking the hydroxy group. Ultrafast time-resolved pump−probe spectroscopy in both the visible and IR region show the occurrence of *E*−*Z* photoisomerization on a 20 ps time scale, similar to the photochemical behavior of DASAs, but on a slower time scale. In contrast to the parent DASA compounds, where the initial photoisomerization is constrained to a single position (next to the hydroxy group), ^{1}H NMR *in situ*-irradiation studies at 213 K reveal that for nonhydroxy DASAs *E*−*Z* photoisomerization can take place at two different bonds, yielding two distinct isomers. These observations are supported by TD-DFT calculations, showing that in the excited state the hydroxy group (pre)selects the neighboring C_2−C_3 bond for isomerization. The TD-DFT analysis also explains the larger solvatochromic shift observed for the parent DASAs as compared to the nonhydroxy analogue, in terms of the dipole moment changes evoked upon excitation. Furthermore, computations provide helpful insights into the photoswitching energetics, indicating that without the hydroxy group the 4π-electrocyclization step is energetically forbidden. Our results establish the central role of the hydroxy group for DASA photoswitching and suggest that its introduction allows for tailoring photoisomerization pathways,

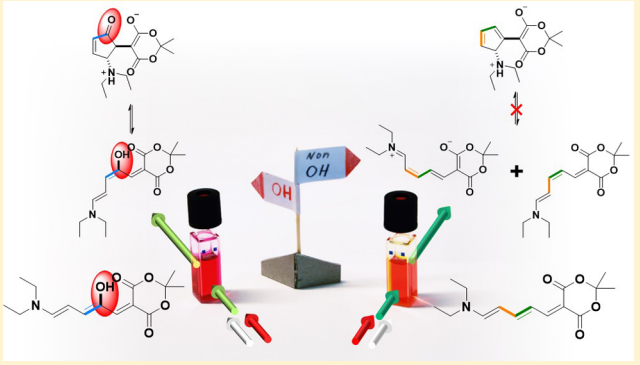

continued...

Received: October 16, 2017
Revised: December 13, 2017
Published: December 24, 2017

DOI: 10.1021/acs.jpca.7b10255
J. Phys. Chem. A 2018, 122, 955−964

presumably both through (steric) fixation via a hydrogen bond with the adjacent carbonyl group of the acceptor moiety, as well as through electronic effects on the polyene backbone. These insights are essential for the rational design of novel, improved DASA photoswitches and for a better understanding of the properties of both DASAs and cyanine dyes.

INTRODUCTION

Polymethine dyes, and more specifically cyanine dyes (Figure 1a),[1] have been used for a plethora of applications, such as material science[2,3] and chemosensing,[4] and continue to be essential for modern cellular biology.[5−7] Hallmarks of this structurally highly diverse class of photochromic molecules include high extinction coefficients, high fluorescence quantum yields and photostability. Since their introduction, they have been used for photography based on silver halides and in optical discs.[2] More recently—together with other fluorescent dyes—they have had a profound impact on cellular biology as labels and fluorescent probes.[8,9] Merocyanines (Figure 1a) have additional properties, including a pronounced solvatochromism and a large change in dipole moment upon excitation, which make them ideal chromophores for developing novel materials for optoelectronics and nonlinear optical applications.[10] They contain donor and acceptor moieties connected by a polyene chain, giving rise to a push−pull system. The charge transfer between donor and acceptor renders them strongly colored and sensitive to the polarity of the environment. Besides being fluorescent, polymethine dyes can undergo *E*−*Z* isomerization and in some cases light-mediated additions of nucleophiles to the polymethine backbone.[11−14] Computationally, these systems are difficult to tackle and have been found to pose quite a challenge in reproducing their spectroscopic properties and correctly estimating their transition energies.[15]

Photoswitches[16] rely on light as an external stimulus to undergo a reversible change in structure, absorption spectrum, dipole moment, polarity, and charge.[17] The possibility of exerting light control over molecular properties enables numerous applications.[18−25] Herein, fluorescence is usually an undesired property (with notable exceptions[26,27]) because it reduces the photochemical quantum yield of isomerization. Recently, donor−acceptor Stenhouse adducts (DASAs) have been introduced (Figure 1).[28,29] DASAs are negative photochromes with a tunable absorption maximum in the visible to near-infrared window. They are easily synthesized and exhibit very little absorption between 300 and 500 nm, a property that has been employed for orthogonal photoswitching.[30] Upon irradiation, the colored elongated triene **A** cyclizes to a colorless form **B** that then thermally opens to give back **A** (Figure 1a). The initially designed DASAs could be reversibly switched in aromatic solvents, but no other organic media, and underwent irreversible cyclization in polar solvents, such as water or methanol.[29] Following investigations on their photochromic behavior,[31−33] structural modifications in both the donor and acceptor moiety have been introduced, aimed at improving their photochromic activity, resulting in second generation photochromes.[34,35] Reversible switching of such derivatives is not limited to aromatic apolar, aprotic solvents and can be extended to solid matrixes (e.g., poly(methyl methacrylate)).[34] Importantly, DASA photoswitches incorporate vital aspects of merocyanine dyes: they are based on a cyclic acceptor (Meldrum's acid or 1,3-dimethylbarbituric acid) connected to a secondary amine-donor through a polyene, with one noticeable difference, the hydroxy group in the C_2 position.

Recent efforts by our group have shed light on the DASA photoswitching mechanism and especially the structural details of the actinic step (Figure 1b).[33,36] Applying a combination of ultrafast spectroscopy and theoretical DFT calculations, the nature of a short-lived intermediate **A′** was identified which is produced following light absorption from DASAs and which allows the system to evolve between the initial elongated triene form **A** and the colorless cyclized form **B** (Figure 1b). The use of time-resolved IR spectroscopic techniques enabled the interpretation of the structural modification induced by light absorption as the result of a photochemical *Z*−*E* isomerization of the C_2−C_3 bond (red, Figure 1b).[36] A subsequent bond rotation around C_3−C_4 (to form **A″**) arranges the molecule's structure to facilitate the formation of the cyclized product **B**. The latter step has been interpreted in terms of a thermal 4π-electrocyclic rearrangement.[29,33,36,37] This mechanism is operative in chlorinated solvents for both first and second generation DASAs, although the time scale and kinetics of the intermediate formation is different between the two families of molecules.[36] The thermal electrocyclization step is reminiscent of both the (aza-)Piancatelli rearrangement,[38−40] as suggested by Read de Alaniz and co-workers[29] and of the *iso*-Nazarov cyclization.[41] De Lera and co-workers have provided an in-depth computational study on the cyclization mechanism of hydroxypentadienyl cations relevant for these type of reactions[37] and suggested an operative electrocyclization mechanism for the polarized pentadienyl cation in favor of an ionic mechanism.

The fundamental understanding of the role of the hydroxy moiety is crucial to elucidate the photochemical differences between DASAs and their related cyanines. To clarify its effect on the polyene chain and its photochemistry, we report here a donor−acceptor Stenhouse adduct lacking the hydroxy group (compound **1**, Figure 1c). Considering the photoswitching mechanism proposed for its parent DASA structure **2**,[33,36] the removal of the OH functionality is likely to prevent the thermal ring closure.[37,42] Indeed, previous photochemical investigations on related merocyanine dyes have shown the occurrence of a photoisomerization reaction, but no observed cyclization.[13,14] Thermal cyclization in the dark is known but only occurs at elevated temperature.[43] Our results confirm these observations and shed further light on the structure−property relationship of both merocyanines and DASAs. Using a combination of time-resolved spectroscopy, in both the visible and IR spectral ranges, NMR *in situ*-irradiation experiments, and theoretical DFT calculations, we have characterized the photochemistry of compound **1** (nonhydroxy DASA, Figure 1c) and compared it with that of compound **2** (parent DASA, Figure 1b). We find that compound **1** undergoes isomerization around bond C_2−C_3 (orange, Figure 1c) but also around C_3−C_4 bond (olive, Figure 1c). This is in contrast to DASAs that were only found to isomerize around C_2−C_3 bond (red, Figure 1b) adjacent to the hydroxy group and to cyclize to form cyclopentenones (**B** form). Time-resolved spectra recorded for compound **1** in both the visible and infrared spectral range, are qualitatively similar to those of the related DASA compound **2**, thus confirming the occurrence of a light-induced isomerization. The time constant for the isomerization process is, however, larger for the nonhydroxy analogue: the process occurs on a 20 ps time scale for compound **1** as compared to a 2 ps time scale observed for compound **2** (in chloroform).[36] Furthermore, compared to that of DASA **2**, the fluorescence increases for compound **1** (Supporting Information section 7).

DOI: 10.1021/acs.jpca.7b10255
J. Phys. Chem. A 2018, 122, 955−964

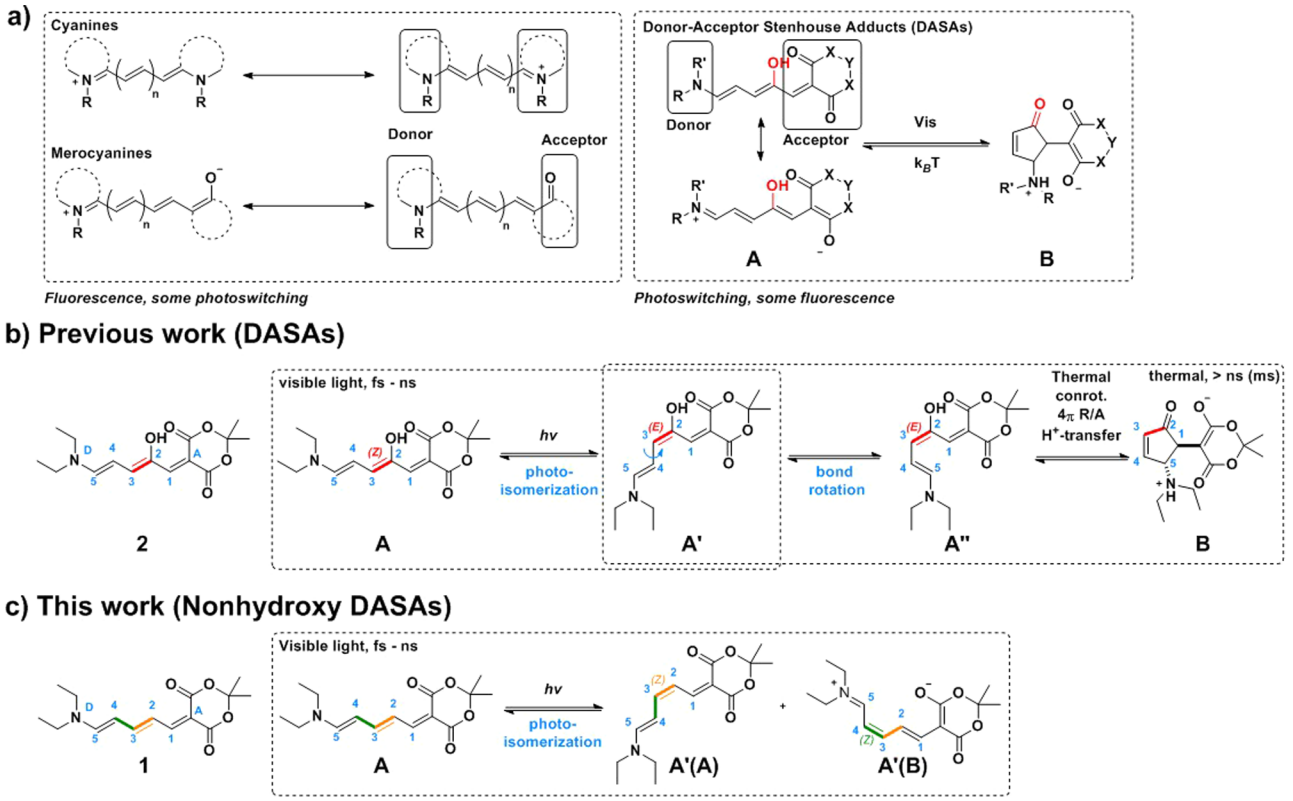

Figure 1. Polymethine dyes and donor−acceptor Stenhouse adducts (DASAs): structural overview (a); proposed photoswitching mechanism of DASAs (b); related DASA compound lacking a hydroxy group (c).

Recently, Qu and co-workers have attached a 1,8-naphthalimide fluorophore to create a DASA-fluorophore conjugate for fluorescence modulation.[44] Taken together, these results show that the hydroxy group in DASAs serves as a "selector" of the bond to isomerize by polarizing the polyene chain weakly in the ground state and strongly in the excited state. The strong hydrogen bond between the hydroxy group and the adjacent carbonyl of the acceptor moiety also prevents large structural distortions in the excited state as well as in the C_3-C_4 bond rotation step (Figure 1b). The latter step eases the formation of the intermediate **A″** that prepares the structure for a ring-closure via a 4π-electrocyclic conrotatory rearrangement. In this step, the presence of the hydroxy group is vital, because it takes part in the proton-transfer process and contributes in stabilizing the charge distribution along the polyene chain driving the electronic rearrangement which ends up with the ring closure reaction.

RESULTS AND DISCUSSION

Steady-State Spectroscopy. To elucidate the responsive switching behavior of DASA **1**, photoisomerization was studied by steady-state spectroscopy (for the synthesis of **1**; see Supporting Information section 2). Figure 2 shows the UV/vis absorption spectra of compound **1** measured in different solvents (Supporting Information section 3) and for comparison the solvatochromic shifts of **2**.

Compared to the spectra of the parent DASA compound **2** (Figure 2c), the absorption band of compound **1** (Figure 2b) undergoes a hypsochromic shift in all solvents, indicating that the removal of the hydroxy functional group increases the gap between the HOMO and LUMO orbitals involved in the S_0-S_1 transition, which are mainly localized on the conjugated triene chain (Figure 3a,b). The observed shifts are in good agreement with theoretical values (e.g., −0.27 eV vs −0.36 eV for toluene; Table S5) obtained by the TD-M06-2X method[45] using the 6-311++G(2df,2p) basis set[46] in combination with the universal continuum solvation model based on solute electron density (SMD)[47] and the corrected linear response (cLR) approach[48] to account for the solvent effects on both ground-state (GS) and excited-state (ES) electron densities. A red shift of the absorption as a function of decreasing polarity is observed among the investigated aprotic solvents, whereas the absorption band appears notably blue-shifted in protic media such as water and methanol. The presence of the protic group in **2** leads to a generally stronger solvatochromism (Figure 2c). The observed trends are again well reproduced by the TD-DFT/cLR/SMD calculations (Table S5). In particular, the stronger solvatochromism of **2** can be rationalized in terms of the changes of the dipole moment upon excitation. Whereas for **1** the change is almost negligible (0.29 D in chloroform), leading to very small solvatochromic shifts, for **2** it is noticeably larger and negative (−1.16 D in chloroform). Consequently, the more polar the solvent is, the more stabilized the GS becomes compared to the ES, leading to larger hypsochromic shifts.

The FTIR spectrum of compound **1** is reported in Figure 4, where the spectrum of **2** is also shown for comparison. Furthermore, Figure 4 reports the simulated FTIR spectra for both molecules obtained at the B3LYP/6-31++G(d,p)/SMD level using the harmonic approximation (fwhm = 12 cm^{-1}; scaling factor 0.98, Supporting Information section 9.2). It can be seen that spectra computed for **A** of both **1** and **2** satisfactorily reproduce all main features of the measured spectra, confirming that both molecules in the ground state attain a similar elongated triene conformation (Supporting Information section 9.1). Analysis of mode composition, as obtained by DFT, suggests that the differences between the FTIR spectra of **1** and **2**, in the reported

DOI: 10.1021/acs.jpca.7b10255
J. Phys. Chem. A 2018, 122, 955−964

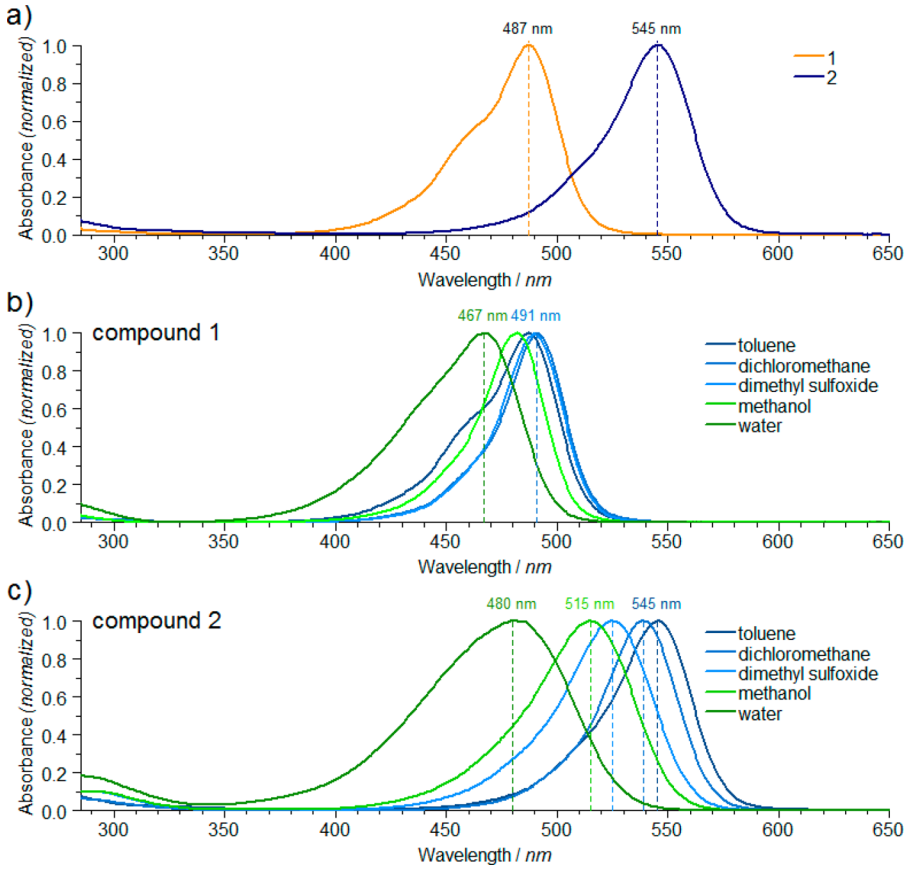

Figure 2. Comparison of UV/vis absorption spectra of compound **1** and **2** in different solvents: (a) compound **1** and **2** in toluene; (b) solvatochromism of compound **1**; (c) solvatochromism of compound **2**.

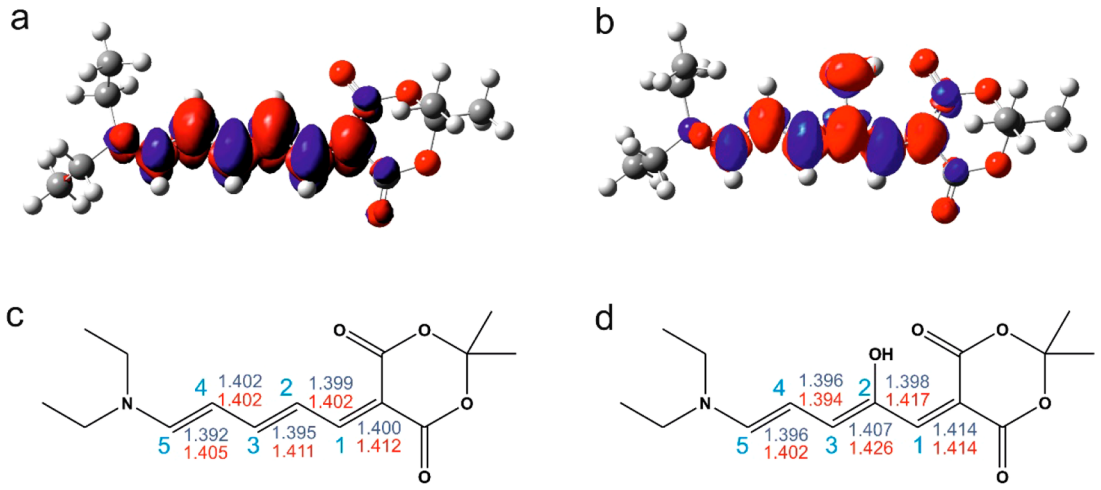

Figure 3. Electronic density difference (EDD) plots between the ES and the GS of **A** for compounds **1** (a) and **2** (b) in chloroform obtained at the M06-2X/6-311++G-2df,2p)/SMD level of theory. The blue (red) regions correspond to a decrease (increase) in electron density upon electronic transition. A contour threshold of 0.001 au has been applied. Bond lengths (Å) are depicted for GS (blue) and ES (red) structures of the **A** form for **1** (c) and **2** (d) in chloroform. GS and ES geometries correspond to geometries optimized at the B3LYP/6-31++G-(d,p)/SMD and D-M06-2X6-31+G-(d)/SMD levels of theory, respectively.

frequency region, mainly arise from a different character of the C−C bonds along the conjugated chain, which is affected by the presence of a hydroxy group, and from the possibility to form a hydrogen bond between the hydroxy group and the acceptor carbonyl group in **2**. Whereas in **1** the bond length alternation indicates efficient π-conjugation, in the case of **2** the $C_{(A)}-C_1$ (A = Acceptor) and C_2-C_3 bonds are noticeably longer (Figure 3c,d). The weakening of these two bonds brings about a small red shift of the 1160 cm^{-1} peak, which mainly accounts for the C_1-C_2/C_2-C_3 asymmetric bond stretching (coupled with the C_4-C_5 stretching and C−H rocking), and also more pronounced shifts of the ca. 1350−1380 and 1500 cm^{-1} bands associated predominantly with the $C_{(A)}-C_1$ stretching and $C_{(A)}-C_1/C_1-C_2$ asymmetric stretching modes, respectively. A significant increase of the intensity of a band at ca. 1500 cm^{-1} is also observed in the case of compound **1**.

DOI: 10.1021/acs.jpca.7b10255
J. Phys. Chem. A 2018, 122, 955−964

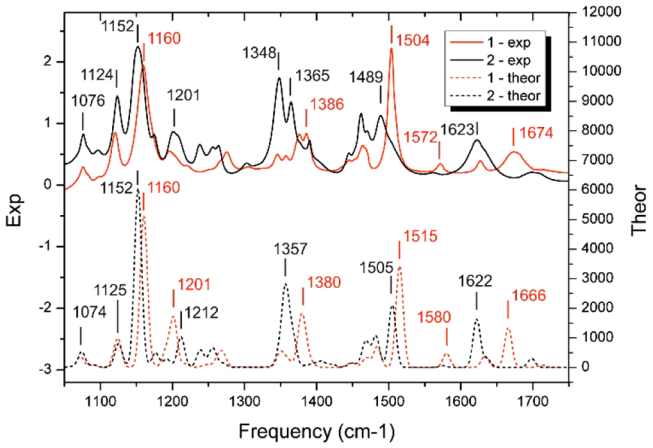

Figure 4. Comparison of the measured (upper) and simulated (lower) FTIR spectra of compound **1** (red line) and **2** (black line) in deuterated chloroform. For the computational details, see the text.

Further differences are noted in the 1600−1700 cm^{-1} region: in particular, the band observed at 1623 cm^{-1} in **2** almost disappears, while a band at 1674 cm^{-1} appears in the spectrum of the nonhydroxy analogue **1**. Our previous DFT analysis of **2** showed that there is a strong H-bond between the OH group linked to the triene chain and one of the carbonyl groups of the acceptor ring.[31,36] ^{1}H NMR spectroscopy confirms the facile exchangeability of this proton (Figure S5). The observed spectral changes in the carbonyl region suggest the assignment of the 1623 cm^{-1} band to the H-bonded ring carbonyl stretch in the case of **2**, which, upon the removal of the hydrogen bond in **1**, blue-shifts to 1675 cm^{-1}, indicating a very strong hydrogen bond. This assignment is further supported by the presence of a band at 1700 cm^{-1} in **2**, due to the second non H-bonded carbonyl. The occurrence of a strong H-bond interaction in DASAs is also evidenced by the inspection of the FTIR spectra of compounds **1** and **2** in the 2500−3500 cm^{-1} region, which show for **2** a broad feature at ca. 2900 cm^{-1} possibly due to the OH-stretch band (Figure S4). As yet, this H-bond has not received extensive attention, but it is clear that it will have mechanistic implications as it will influence the proton-transfer step to form the zwitterionic structure **B** shown in Figure 1b for the first generation DASA **2**. From this point of view, studies of DASA derivatives in which the strength of such a hydrogen bond can be modulated would be highly interesting.

To assess the usefulness of **1** as photoswitch, UV/vis spectroscopy with irradiation under steady-state conditions was performed (Figure 5, Supporting Information section 6). No photobleaching of the sample is observed upon irradiation, as would be the case for **2**. However, a photostationary state is rapidly reached and maintained under irradiation. After irradiation is stopped, rapid relaxation is observed. A bathochromically shifted absorption band is temporarily apparent, reminiscent of the intermediate formed in the photoswitching of **2**.[33] Solvent-polarity influences the extent of this red-shift (Supporting Information sections 6 and 7). Compound **1** shows clean photoswitching throughout a range of solvents (toluene, dichloromethane, chloroform, methanol, dimethyl sulfoxide, acetone, water, and PBS buffer), with very little fatigue observed in aqueous environments.

Time-Resolved Spectroscopy. Time-resolved spectroscopy allows detailed insights into the structure and dynamics of the compound in question during the actinic step. The EADS (evolution-associated difference spectra) obtained by global analysis[49] of visible pump−probe data recorded for compound **1**

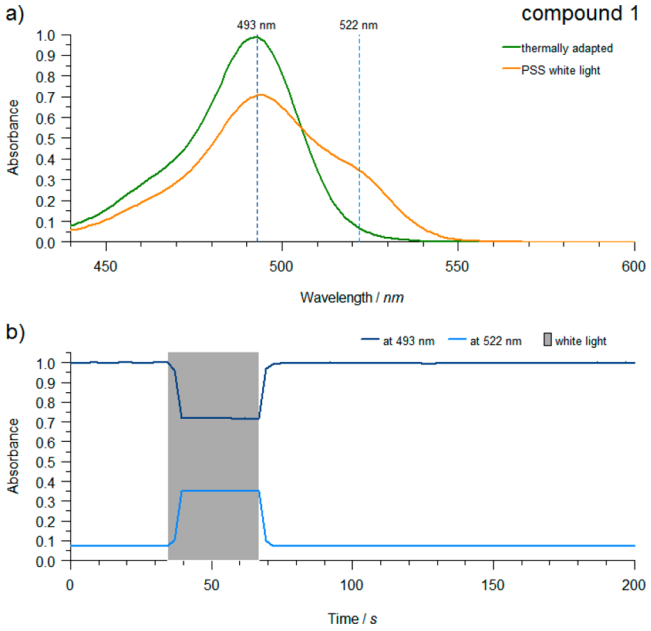

Figure 5. a) Absorption spectra for the photoisomerization of compound **1** (λ_{max} = 493 nm; ∼6 μM in chloroform; 293 K; optical cutoff filter <440 nm, SCF-50S-44Y) with white light (Thorlabs, OSL1-EC, PSS = photostationary state) and (b) corresponding time evolution observed at 493 and 522 nm. The shaded area indicates the irradiation period.

in chloroform upon λ = 480 nm light excitation (Supporting Information section 8) are shown in Figure 6. As evidenced from photoaccumulation experiments (Figure 5, Supporting Information section 6), the sample does not cyclize irrespective of the solvent. Nonetheless, a long-lived bathochromically shifted band peaking at 512 nm appears in the transient spectra ca. 20 ps after light absorption and it closely resembles that assigned to the *Z*−*E* isomerized intermediate (**A′**) observed in the parent DASA **2**.[33] The EADS shown in Figure 6 closely follow those reported for DASA **2**.[36] As noticed from inspection of Figure 6, in chloroform a bleaching band peaked at 500 nm, promptly appears upon photoexcitation. The signal intensity partially recovers in 2 ps; then, on a time scale of 20 ps, a positive band, peaking at 512 nm, appears in the transient spectra (see the blue EADS component reported in Figure 6a). The EADS obtained from transient absorption measurements repeated in different solvents are reported in the Supporting Information (Figure S34). The qualitative appearances of the transient signal and the observed spectral evolution do not significantly change when the solvent is changed. In all cases, a positive band peaking at 500−515 nm is observed in the long-lived spectral component. However, the maximum absorption band of the photoproduct and the observed shift with respect to the ground-state absorption both depend on the solvent. This explains why in methanol, where the ground-state absorption band is very broad, a bathochromically shifted band is hardly seen in steady-state photoaccumulation experiments (Supporting Information section 6.4). The quantum yields for the photoisomerization of **1** estimated from the ultrafast measurements are 6% (toluene), 11.9% (dichloromethane), 13.8% (chloroform), 8.6% (methanol), and 7% (dimethyl sulfoxide).

The dynamics of photoproduct formation is influenced by solvent polarity. A comparison of the kinetic traces recorded at the maximum absorption of the photogenerated species is reported in Figure 6b, showing that the rate of appearance of the positive peak in the transient spectra slows down upon increasing

DOI: 10.1021/acs.jpca.7b10255
J. Phys. Chem. A 2018, 122, 955−964

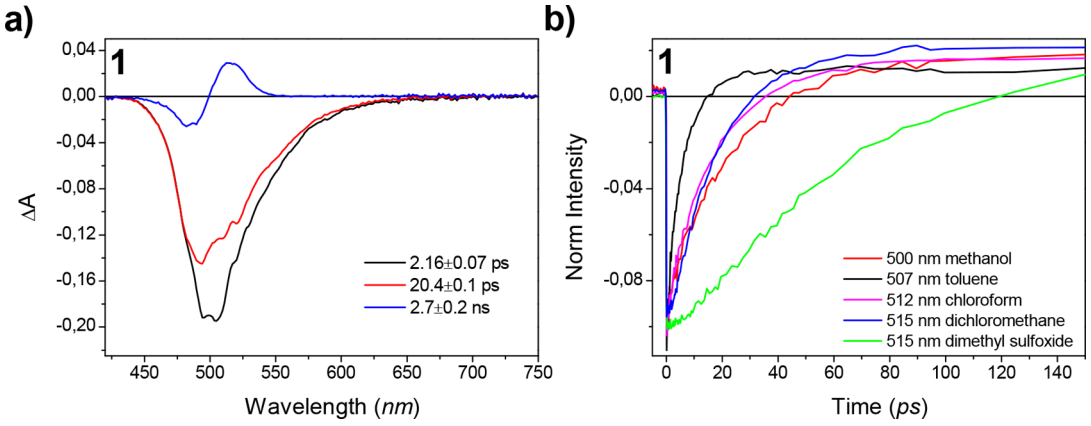

Figure 6. (a) EADS obtained from global analysis[49] of time-resolved visible pump−probe data recorded for compound **1** dissolved in chloroform and excited at 480 nm. (b) Kinetic traces recorded on the maximum of the product band in various solvents.

the polarity of the solvent. The time constant for the photoproduct formation is in fact 8.5 ps in toluene and increases to 56 ps in dimethyl sulfoxide, where, besides a polarity effect, also the increased viscosity could play a role. It is, however, worth noticing that even in the case of toluene the photoproduct is formed with a slower rate than for the parent DASA molecule **2** (in that case the intermediate is observed on a 2 ps time scale) and no further spectral evolution of the product band is observed in any solvent.

To further characterize the nature of the photoproduct obtained upon light absorption for compound **1**, picosecond transient infrared spectra were recorded. IR-based techniques are particularly suited to shed light on changes occurring in molecular structures upon photoexcitation and have been widely used to investigate light induced structural changes in polyene systems.[50−52] The EADS obtained from global analysis[49] of transient spectra acquired between 1100 and 1750 cm^{-1} are reported in Figure 7. In the case of transient infrared measurements the sample has been excited on the red edge of its absorption band, at 510 nm.

The initial spectral component (black EADS in Figure 7a) shows several negative bands, whose position well corresponds to the bleaching of ground-state modes. As already noticed in the case of the previously studied DASA photoswitches, very few excited-state absorption bands are observed.[36] DFT calculations of the vibrational spectra in the excited state have shown a strong decrease of intensity of almost all the vibrational bands occurring in the excited state, and only minor shifts compared with ground-state band positions, which explains the predominance of negative signals in the transient spectrum.[36] In the carbonyl stretching region (1600−1750 cm^{-1}), the excited-state bands are clearly visible. In this region, three positive signals at 1606, 1635, and 1694 cm^{-1} are observed. On a 7 ps time scale, the intensity of the bleaching signals decreases, while the observable positive bands slightly sharpen and blue-shift. This spectral behavior allows assigning the 7 ps component to vibrational cooling in the excited state. The initial evolution appears to be slower than what is observed in transient visible measurements, which may be due to the different excitation conditions used in this case, preventing excess vibrational energy in the S_1 state. The following evolution, occurring on a 21.5 ps time scale, is associated with a further recovery of the bleaching signals and to the appearance of a few more positive bands. In particular, small absorption bands at 1190, 1236 1340, and 1421 cm^{-1} develop (Figure 7b). The spectrum of the long-living spectral component extracted from the globally analyzed time-resolved data of compound **1** resembles that observed for the parent DASA photoswitch **2**[36] and is assigned to a photogenerated intermediate resulting from *E*−*Z* isomerization. In the present case, however, two positive bands are noticed in the 1190−1240 cm^{-1} region. Moreover, the differential signal at 1160(−)/1190(+) cm^{-1} is less pronounced if compared to that observed for compound **2**, possibly because the negative signal is in this case much broader. DFT simulations reproduce all main features of the observed spectrum (Figure 7c), except for predicting a negative signal at ca. 1200 cm^{-1}, which is a consequence of an overestimated absorption intensity of **A** in its GS (cf. Figure 4). Nevertheless, the similarity between the spectral evolutions of the transient infrared signal of compounds **1** and **2** leads us to conclude that the photoproducts obtained in systems with and without the OH functionality have similar natures and result from a photoisomerization event.

^{1}H NMR *in Situ*-Irradiation Experiments. The structure of the photoproduct has been further investigated by performing NMR *in situ*-irradiation studies at low temperature (203-213 K). Notably, irradiation (470 nm LED, Thorlabs, M470F3) of **1** at 213 K in deuterated dichloromethane (Supporting Information section 10.1.1) leads to the reversible formation of two isomers **A′(A)** and **A′(B)** (Figure 8). Full structural assignment of these two isomers was performed in deuterated acetone (Supporting Information section 10.1.2) due to overlapping NMR signals of isomer **A′(B)** with the parent compound **1** in deuterated dichloromethane (Figure S49). 2D-NMR spectroscopy under irradiation (^{1}H,^{1}H-COSY, ^{1}H,^{1}H-TOCSY and 2D-NOESY) and analysis of the coupling constants between the polyene protons suggest a comparable behavior of **1** in deuterated dichloromethane and deuterated acetone (Supporting Information sections 10.1.1 and 10.1.2), which is also observed by UV/vis spectroscopy (Supporting Information sections 6.2 and 6.6). Although coupling constants in the parent compound are in the range 11−14 Hz indicative of a linear, elongated configuration, lower coupling constants (<10 Hz) strongly suggest a *Z*-configuration for **1** after photoisomerization. We thus conclude that the two isomers **A′(A)** and **A′(B)** differ in the position of the *Z*-bond within the polyene chain (C_2−C_3 vs C_3−C_4). This is supported by the through-space connectivity deduced from nuclear Overhauser spectroscopy (Supporting Information sections 10.1.1.5 and 10.1.2.4). For clarity, **A′(B)** is drawn in its resonance form, noting the partial double bond character throughout the conjugated system (see discussion of bond lengths above). Upon cessation of irradiation, both isomers revert back to **A**. The fact that two independent isomers are formed is remarkable, as for DASA **2** only one isomer is formed

DOI: 10.1021/acs.jpca.7b10255
J. Phys. Chem. A 2018, 122, 955−964

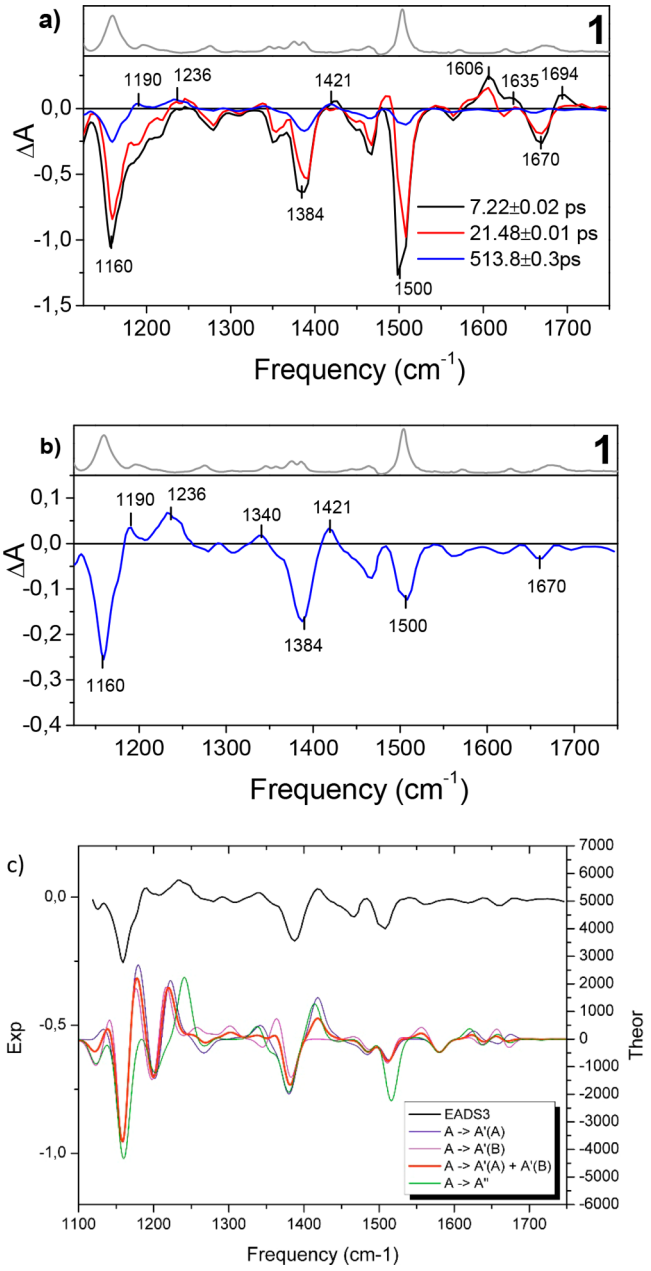

Figure 7. (a) EADS obtained from global analysis[49] of time-resolved infrared data recorded for compound **1** in deuterated chloroform. The last spectral component is magnified in panel b. The gray line in the top panel of the figure reports the FTIR spectrum of the molecule in the same solvent. (c) Comparison of experimental and simulated last EADS components in the same solvent. The blue/pink/red/green lines correspond to the GS difference harmonic IR spectra of the species **A′(A)**/**A′(B)**/**A′(A)**+**A′(B)**(1:1)/**A″** with respect to the spectrum of **A** obtained at the B3LYP/6-31++G-(d,p)/SMD level of theory (fwhm = 20 cm^{-1}, scaling factor = 0.98).

under otherwise identical conditions (deuterated dichloromethane, 213 K, 530 nm LED, Thorlabs, M530F2).[33] The hydroxy group thus seems to (pre)select the bond to be isomerized (C_2−C_3) and to suppress isomerization of the C_3−C_4 bond (Figure 1). Electronic density difference (EDD) plots and analysis of bond-length alternations (Figure 3) support this observation. As the isomers are red-shifted with respect to **A** (Supporting Information section 6.6), irradiation near their absorption maximum should accelerate their back-isomerization to **A**. Irradiation of the sample with 530 nm (LED, Thorlabs, M530F2) indeed accelerates the back-relaxation to **A** (Supporting Information section 10.1.2.6). Temperature-dependent ^{1}H NMR (Supporting Information section 10.3) and UV/vis studies (Supporting Information section 10.4) show different thermal behavior of the two isomers, accounting for the observed change in photostationary states achieved under irradiation at different temperatures, and different rates of thermal relaxation. Although **A′(B)** dominates over **A′(A)** in steady-state concentration under irradiation at 213 K in acetone-d_6, the ratio changes in favor of **A′(A)** with increasing temperature, leading to an almost disappearing signal of **A′(B)** at 233 K (Figure S79 and S81).

TD-DFT calculations support these findings. The computed energies for ground and excited states of the various isomers and the transition states for the interconversion between the different species are summarized in Table S4. The photoisomerizations are likely to be reversible as was previously shown for DASA **2**.[36] Importantly, the thermal stability of the isomers (especially of **A′(A)**) lies in the range of what was observed before for **2**.[33] Given the calculated energies, the formation of **A″** could potentially be possible. However, none of the employed spectroscopic measurements (NMR, TRIR) indicates that this is actually occurring.

To rationalize the lack of cyclization from compound **1**, we analyzed the change of bond lengths and charge distribution during the transformation from **A** to **B** (Supporting Information section 9.1). Our calculations show that the presence of the hydroxy group is essential to polarize the polyene chain in the correct way to drive cyclization, once the molecule reaches the **A″** configuration. Furthermore, because a proton transfer is expected to take place during cyclization, the activation barrier for the proton-transfer cyclization step for compounds **1** and **2** was estimated (Figure 9). Two potential energy curves along the reaction coordinate related to the C_1−C_5 interatomic distance have been calculated at the B3LYP/6-31+G-(d)/SMD level by constrained optimizations of all coordinates, with the C_1−C_5 bond length kept frozen, using methanol as a typical protic environment (Figure 9). The green curves shown in Figure 9 describe the ring closure in the **A″** form, and the blue curves refer to the ring opening in the **B** form. The crossing point of the two curves enables us to estimate a barrier for intermolecular proton transfer (mediated by protic solvent). It can be seen that the barrier for cyclization of compound **1** is very high (ca. 34 kcal/mol). However, in the case of compound **2** the presence of the hydroxy group clearly facilitates the proton transfer and electrocyclization, decreasing the activation barrier to ca. 26 kcal/mol. A proton-transfer step is important, as Stenhouse salts lacking such a strong hydrogen bond show strongly pH-dependent photoswitching.[42] In addition, our calculations suggest that the presence of the OH stabilizes a partial positive charge on carbon C_5 and a small negative charge on carbon C_1, favoring the ring closure step (Supporting Information section 9.1). This is not possible for compound **1**, lacking the hydroxy group, majorly contributing to the observed higher barrier for cyclization of **1** as compared to **2**.

■ CONCLUSIONS

The presented experimental and theoretical analyses have elucidated the important role of the hydroxy substituent on the DASA photoswitching capacity, focusing in particular on the intermediate products originating from the actinic step. Our experimental and theoretical work shows that the group acts by restricting photoisomerization of compound **2** toward the sole formation of isomer **A′(A)**. The "preselection" of bond C_2−C_3 is likely due to

DOI: 10.1021/acs.jpca.7b10255
J. Phys. Chem. A 2018, 122, 955−964

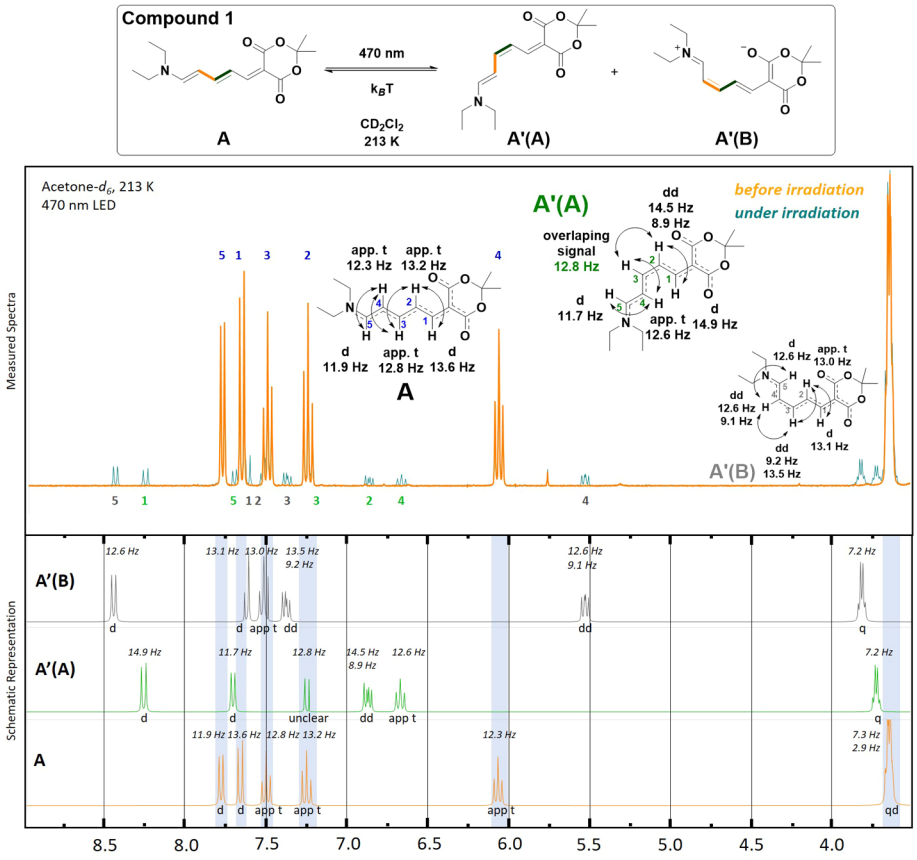

Figure 8. NMR *in situ*-irradiation experiments of compound **1** reveal two sets of photogenerated peaks corresponding to isomers **A′(A)** (green) and **A′(B)** (gray). Acetone-d_6 was used to verify the coupling constants, as in deuterated dichloromethane some signals were overlapping. Formation of **A′(A)** and **A′(B)** isomers is reversible and light-dependent. A schematic representation of the relevant spectra (obtained by line fitting) is provided for clarity.

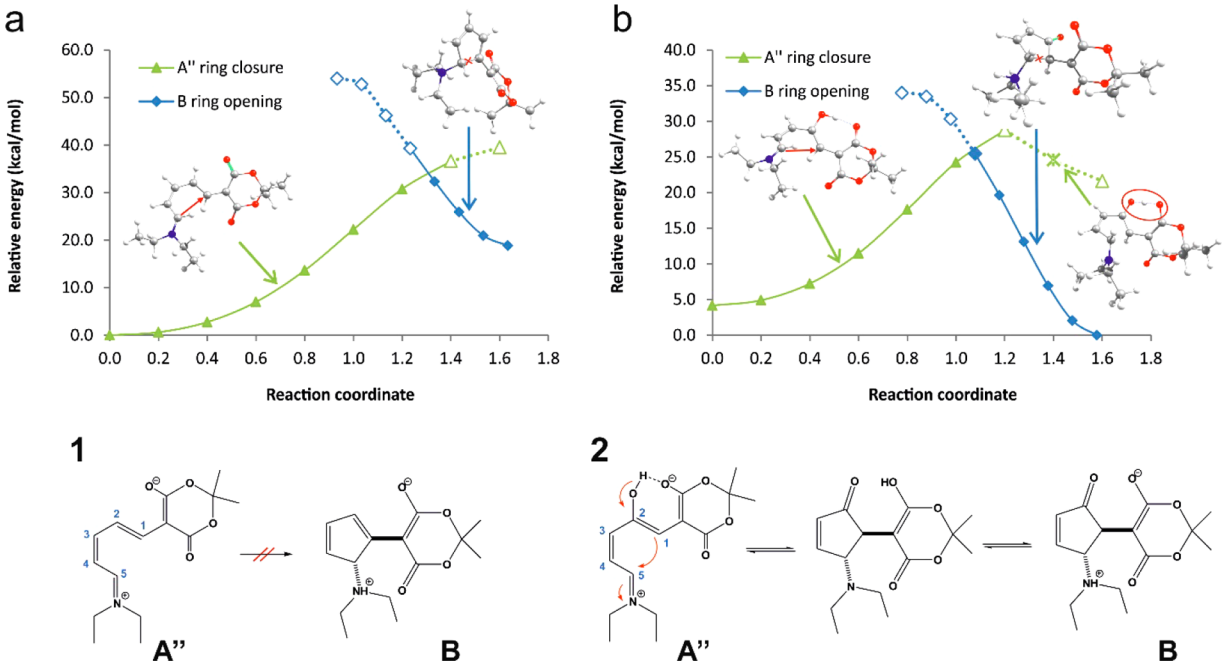

Figure 9. Potential energy curves for the proton-transfer cyclization step, i.e., **A″** to **B** transformation for compounds **1** (a) and **2** (b) computed at the B3LYP/6-31+G-(d)/SMD level of theory. The green curve corresponds to the ring closure in the **A″** form, and the blue curve corresponds to the ring opening starting from the **B** form. The reaction coordinate (Å) is defined as the negative relative distance of carbon atoms with respect to the equilibrium $C_1\cdots C_5$ bond distance in **A″**. The crossing point of the green and blue curves indicates the barrier for intermolecular proton transfer. The star point on the green curve in (b) corresponds to an intramolecular proton-transfer configuration. The fact that it is positioned behind the crossing point implies that H^+ is preferentially transferred to the environment or to a neighboring DASA molecule. See also analysis of bond lengths and charge redistribution during the cyclization step in Supporting Information section 9.1.

DOI: 10.1021/acs.jpca.7b10255
J. Phys. Chem. A 2018, 122, 955−964

a decreased electron density and elongation of that particular bond (particularly in the ES). Notably, in the case of the nonhydroxy analogue **1**, two isomers **A′(A)** and **A′(B)** are formed at low temperature under irradiation in photoaccumulation experiments as observed by NMR spectroscopy.

Time-resolved UV/vis and IR spectroscopy have provided spectroscopic insights into details and time scales of the isomerization pathway. They fully support the occurrence of an *E*−*Z* isomerization upon photoexcitation and support the formation of two photoswitched isomers, although the similarity of the DFT-predicted IR spectra of **A′(A)** and **A′(B)** impedes an unambiguous distinction of the two isomers. The comparison of the photoisomerization kinetics of **1** and **2** shows that the nonhydroxy analogue **1** isomerizes about 10 times slower than the parent DASA. The increased photoisomerization rate observed for compound **2** can be rationalized in terms of the influence that the hydroxy substituent has on the triene bond length alternation and through steric effects. A somehow related effect has been previously observed in the case of the rhodopsin chromophore, where the introduction of a methyl substituent accelerates the photoisomerization rate in solution.[53,54] Overall, our results show that by introducing a hydroxy group in the C_2-position of the polyene chain one can control photoswitching pathways and favor cyclization. The role of the strong hydrogen-bond in the proton-transfer step leading to **B** in compound **2** is of considerable interest but needs further study.

The presented results are directly applicable for improvements of DASA photoswitching and are important for acquiring a better understanding of the (photo)chemical properties of DASAs and cyanine dyes. One particularly attractive approach includes the substitution of the hydroxy group with other polar protic groups such as thiols and amines or polarizing groups such as halides, and varying the position of these groups. Such studies are presently being pursued.

■ ASSOCIATED CONTENT

Supporting Information

This information is available via the Internet at The Supporting Information is available free of charge on the ACS Publications website at DOI: 10.1021/acs.jpca.7b10255.

Experimental procedures and characterization of compounds, UV/vis absorption spectra and photoswitching studies in different solvents, fluorescence spectra, FTIR spectra and ultrafast visible and mid-IR spectroscopy; EADS (evolution associated difference spectra) obtained by global analysis; TD-DFT computations and NMR *in situ* irradiation experiments (PDF)

■ AUTHOR INFORMATION

Corresponding Authors

*M.D.D. E-mail: didonato@lens.unifi.it.
*B.L.F. E-mail: b.l.feringa@rug.nl.

ORCID

Michael M. Lerch: 0000-0003-1765-0301
Adèle D. Laurent: 0000-0001-9553-9014
Wiktor Szymański: 0000-0002-9754-9248
Mariangela Di Donato: 0000-0002-6596-7031
Ben L. Feringa: 0000-0003-0588-8435

Author Contributions

The manuscript was written through contributions of all authors. All authors have given approval to the final version of the manuscript.

Notes

The authors declare no competing financial interest.

■ ACKNOWLEDGMENTS

The authors gratefully acknowledge financial support from Laserlab-Europe (LENS002289), the Ministry of Education, Culture and Science (Gravitation program 024.001.035), The Netherlands Organization for Scientific Research (NWO−CW, Top grant to B.L.F., VIDI grant no. 723.014.001 for W.S.), the European Research Council (Advanced Investigator Grant, no. 227897 to B.L.F.) and the Royal Netherlands Academy of Arts and Sciences Science (KNAW). M.M. acknowledges the Czech Science Foundation (project no. 16-01618S), the Ministry of Education, Youth and Sports of the Czech Republic (grant LO1305) and the Grant Agency of the Slovak Republic (VEGA project No. 1/0737/17). This research used computational resources of (1) the GENCI-CINES/IDRIS, (2) CCIPL (Centre de Calcul Intensif des Pays de Loire), (3) a local Troy cluster, and (4) the HPCC of the Matej Bel University in Banska Bystrica by using the infrastructure acquired in projects ITMS 26230120002 and 26210120002 supported by the Research and Development Operational Programme funded by the ERDF. The Swiss Study Foundation is acknowledged for a fellowship to M.M.L. We thank P. van der Meulen for support with the temperature dependent NMR *in situ* irradiation studies and T. Tiemersma-Wegman for ESI-MS analyses.

■ REFERENCES

(1) Shindy, H. A. Fundamentals in the Chemistry of Cyanine Dyes: A Review. *Dyes Pigm.* **2017**, *145*, 505−513.
(2) Mishra, A.; Behera, R. K.; Behera, P. K.; Mishra, B. K.; Behera, G. B. Cyanines during the 1990s: A Review. *Chem. Rev.* **2000**, *100* (6), 1973−2011.
(3) Fabian, J.; Nakazumi, H.; Matsuoka, M. Near-Infrared Absorbing Dyes. *Chem. Rev.* **1992**, *92* (6), 1197−1226.
(4) Sun, W.; Guo, S.; Hu, C.; Fan, J.; Peng, X. Recent Development of Chemosensors Based on Cyanine Platforms. *Chem. Rev.* **2016**, *116* (14), 7768−7817.
(5) *Heterocyclic Polymethine Dyes*; Strekowski, L., Ed.; Topics in Heterocyclic Chemistry; Springer: Berlin, Heidelberg, 2008; Vol. *14*.
(6) Guo, Z.; Park, S.; Yoon, J.; Shin, I. Recent Progress in the Development of Near-Infrared Fluorescent Probes for Bioimaging Applications. *Chem. Soc. Rev.* **2014**, *43* (1), 16−29.
(7) Lavis, L. D.; Raines, R. T. Bright Building Blocks for Chemical Biology. *ACS Chem. Biol.* **2014**, *9* (4), 855−866.
(8) Gonçalves, M. S. T. Fluorescent Labeling of Biomolecules with Organic Probes. *Chem. Rev.* **2009**, *109* (1), 190−212.
(9) *The Molecular Probes Handbook. A Guide to Fluorescent Probes and Labeling Technologies*, 11th ed.; Johnson, I. D., Spence, M. T. Z., Eds.; Life Technologies Corporation, 2010.
(10) Kulinich, A. V.; Ishchenko, A. A. Merocyanine Dyes: Synthesis, Structure, Properties and Applications. *Russ. Chem. Rev.* **2009**, *78* (2), 141−164.
(11) Dempsey, G. T.; Bates, M.; Kowtoniuk, W. E.; Liu, D. R.; Tsien, R. Y.; Zhuang, X. Photoswitching Mechanism of Cyanine Dyes. *J. Am. Chem. Soc.* **2009**, *131* (51), 18192−18193.
(12) Vaughan, J. C.; Dempsey, G. T.; Sun, E.; Zhuang, X. Phosphine Quenching of Cyanine Dyes as a Versatile Tool for Fluorescence Microscopy. *J. Am. Chem. Soc.* **2013**, *135* (4), 1197−1200.
(13) Aramendia, P. F.; Krieg, M.; Nitsch, C.; Bittersmann, E.; Braslavsky, S. E. The Photophysics of Merocyanine 540. A Comparative Study in Ethanol and in Liposomes. *Photochem. Photobiol.* **1988**, *48* (2), 187−194.
(14) Benniston, A. C.; Harriman, A.; Gulliya, K. S. Photophysical Properties of Merocyanine 540 Derivatives. *J. Chem. Soc., Faraday Trans.* **1994**, *90* (7), 953−961.

(15) Le Guennic, B.; Jacquemin, D. Taking Up the Cyanine Challenge with Quantum Tools. *Acc. Chem. Res.* **2015**, *48* (3), 530−537.
(16) *Molecular Switches*, 2nd ed.; Feringa, B. L., Browne, W. R., Eds.; Wiley-VCH: Weinheim, Germany, 2011.
(17) Brieke, C.; Rohrbach, F.; Gottschalk, A.; Mayer, G.; Heckel, A. Light-Controlled Tools. *Angew. Chem., Int. Ed.* **2012**, *51* (34), 8446−8476.
(18) Russew, M. M.; Hecht, S. Photoswitches: From Molecules to Materials. *Adv. Mater.* **2010**, *22* (31), 3348−3360.
(19) de Silva, A. P. *Molecular Logic-Based Computation, Monographs in Supramolecular Chemistry*; RSC Publishing, 2012.
(20) Klajn, R. Spiropyran-Based Dynamic Materials. *Chem. Soc. Rev.* **2014**, *43* (1), 148−184.
(21) Natali, M.; Giordani, S. Molecular Switches as Photocontrollable "Smart" Receptors. *Chem. Soc. Rev.* **2012**, *41* (10), 4010−4029.
(22) Szymański, W.; Beierle, J. M.; Kistemaker, H. A. V.; Velema, W. A.; Feringa, B. L. Reversible Photocontrol of Biological Systems by the Incorporation of Molecular Photoswitches. *Chem. Rev.* **2013**, *113* (8), 6114−6178.
(23) Velema, W. A.; Szymanski, W.; Feringa, B. L. Photopharmacology: Beyond Proof of Principle. *J. Am. Chem. Soc.* **2014**, *136* (6), 2178−2191.
(24) Broichhagen, J.; Frank, J. A.; Trauner, D. A Roadmap to Success in Photopharmacology. *Acc. Chem. Res.* **2015**, *48* (7), 1947−1960.
(25) Erbas-Cakmak, S.; Leigh, D. A.; McTernan, C. T.; Nussbaumer, A. L. Artificial Molecular Machines. *Chem. Rev.* **2015**, *115* (18), 10081−10206.
(26) Yun, C.; You, J.; Kim, J.; Huh, J.; Kim, E. Photochromic Fluorescence Switching from Diarylethenes and Its Applications. *J. Photochem. Photobiol., C* **2009**, *10* (3), 111−129.
(27) Irie, M.; Fukaminato, T.; Sasaki, T.; Tamai, N.; Kawai, T. A Digital Fluorescent Molecular Photoswitch. *Nature* **2002**, *420* (6917), 759−760.
(28) Helmy, S.; Leibfarth, F. A.; Oh, S.; Poelma, J. E.; Hawker, C. J.; De Alaniz, J. R. Photoswitching Using Visible Light: A New Class of Organic Photochromic Molecules. *J. Am. Chem. Soc.* **2014**, *136* (23), 8169−8172.
(29) Helmy, S.; Oh, S.; Leibfarth, F. A.; Hawker, C. J.; Read De Alaniz, J. Design and Synthesis of Donor-Acceptor Stenhouse Adducts: A Visible Light Photoswitch Derived from Furfural. *J. Org. Chem.* **2014**, *79* (23), 11316−11329.
(30) Lerch, M. M.; Hansen, M. J.; Velema, W. A.; Szymanski, W.; Feringa, B. L. Orthogonal Photoswitching in a Multifunctional Molecular System. *Nat. Commun.* **2016**, *7*, 12054.
(31) Laurent, A. D.; Medveď, M.; Jacquemin, D. Using Time-Dependent Density Functional Theory to Probe the Nature of Donor−Acceptor Stenhouse Adduct Photochromes. *ChemPhysChem* **2016**, *17* (12), 1846−1851.
(32) Belhboub, A.; Boucher, F.; Jacquemin, D. An Ab Initio Investigation of Photoswitches Adsorbed onto Metal Oxide Surfaces: The Case of Donor−acceptor Stenhouse Adduct Photochromes on TiO_2 Anatase. *J. Mater. Chem. C* **2017**, *5* (7), 1624−1631.
(33) Lerch, M. M.; Wezenberg, S. J.; Szymanski, W.; Feringa, B. L. Unraveling the Photoswitching Mechanism in Donor-Acceptor Stenhouse Adducts. *J. Am. Chem. Soc.* **2016**, *138* (20), 6344−6347.
(34) Hemmer, J. R.; Poelma, S. O.; Treat, N.; Page, Z. A.; Dolinski, N. D.; Diaz, Y. J.; Tomlinson, W.; Clark, K. D.; Hooper, J. P.; Hawker, C.; et al. Tunable Visible and Near Infrared Photoswitches. *J. Am. Chem. Soc.* **2016**, *138* (42), 13960−13966.
(35) Mallo, N.; Brown, P. T.; Iranmanesh, H.; MacDonald, T. S. C.; Teusner, M. J.; Harper, J. B.; Ball, G. E.; Beves, J. E. Photochromic Switching Behaviour of Donor−acceptor Stenhouse Adducts in Organic Solvents. *Chem. Commun.* **2016**, *52* (93), 13576−13579.
(36) Di Donato, M.; Lerch, M. M.; Lapini, A.; Laurent, A. D.; Iagatti, A.; Bussotti, L.; Ihrig, S. P.; Medved′, M.; Jacquemin, D.; Szymański, W.; et al. Shedding Light on the Photoisomerization Pathway of Donor-Acceptor Stenhouse Adducts. *J. Am. Chem. Soc.* **2017**, *139* (44), 15596−15599.
(37) Nieto Faza, O.; Silva López, C.; Álvarez, R.; De Lera, Á. R. Theoretical Study of the Electrocyclic Ring Closure of Hydroxypentadienyl Cations. *Chem. - Eur. J.* **2004**, *10* (17), 4324−4333.
(38) Piancatelli, G.; Scettri, A.; Barbadoro, S. A Useful Preparation of 4-Substituted 5-Hydroxy-3-Oxocyclopentene. *Tetrahedron Lett.* **1976**, *17* (39), 3555−3558.
(39) Piutti, C.; Quartieri, F. The Piancatelli Rearrangement: New Applications for an Intriguing Reaction. *Molecules* **2013**, *18* (10), 12290−12312.
(40) Veits, G. K.; Wenz, D. R.; Read De Alaniz, J. Versatile Method for the Synthesis of 4-Aminocyclopentenones: Dysprosium(III) Triflate Catalyzed Aza-Piancatelli Rearrangement. *Angew. Chem., Int. Ed.* **2010**, *49* (49), 9484−9487.
(41) Riveira, M. J.; Marsili, L. A.; Mischne, M. P. The *Iso*-Nazarov Reaction. *Org. Biomol. Chem.* **2017**, *15*, 9255−9274.
(42) Honda, K.; Komizu, H.; Kawasaki, M. Reverse Photocharomism of Stenhouse Salts. *J. Chem. Soc., Chem. Commun.* **1982**, *4*, 253.
(43) McNab, H.; Monahan, L. C.; Gray, T. Thermal Cyclisation Reactions of Vinylogous Aminomethylene Meldrum's Acid Derivatives. *J. Chem. Soc., Chem. Commun.* **1987**, *0* (3), 140−141.
(44) Yang, S.; Liu, J.; Cao, Z.; Li, M.; Luo, Q.; Qu, D. Fluorescent Photochromic Donor-Acceptor Stenhouse Adduct Controlled by Visible Light. *Dyes Pigm.* **2018**, *148*, 341−347.
(45) Zhao, Y.; Truhlar, D. G. The M06 Suite of Density Functionals for Main Group Thermochemistry, Thermochemical Kinetics, Noncovalent Interactions, Excited States, and Transition Elements: Two New Functionals and Systematic Testing of Four M06-Class Functionals and 12 Other Function. *Theor. Chem. Acc.* **2008**, *120* (1−3), 215−241.
(46) Ditchfield, R.; Hehre, W. J.; Pople, J. A. Self-Consistent Molecular-Orbital Methods. IX. An Extended Gaussian-Type Basis for Molecular-Orbital Studies of Organic Molecules. *J. Chem. Phys.* **1971**, *54* (2), 724−728.
(47) Marenich, A. V.; Cramer, C. J.; Truhlar, D. G. Universal Solvation Model Based on Solute Electron Density and on a Continuum Model of the Solvent Defined by the Bulk Dielectric Constant and Atomic Surface Tensions. *J. Phys. Chem. B* **2009**, *113* (18), 6378−6396.
(48) Caricato, M.; Mennucci, B.; Tomasi, J.; Ingrosso, F.; Cammi, R.; Corni, S.; Scalmani, G. Formation and Relaxation of Excited States in Solution: A New Time Dependent Polarizable Continuum Model Based on Time Dependent Density Functional Theory. *J. Chem. Phys.* **2006**, *124* (12), 124520.
(49) Van Stokkum, I. H. M.; Larsen, D. S.; Van Grondelle, R. Global and Target Analysis of Time-Resolved Spectra. *Biochim. Biophys. Acta, Bioenerg.* **2004**, *1657* (2−3), 82−104.
(50) Di Donato, M.; Ragnoni, E.; Lapini, A.; Foggi, P.; Hiller, R. G.; Righini, R. Femtosecond Transient Infrared and Stimulated Raman Spectroscopy Shed Light on the Relaxation Mechanisms of Photo-Excited Peridinin. *J. Chem. Phys.* **2015**, *142* (21), 212409.
(51) Ragnoni, E.; Di Donato, M.; Iagatti, A.; Lapini, A.; Righini, R. Mechanism of the Intramolecular Charge Transfer State Formation in All-Trans-β-Apo-8′-Carotenal: Influence of Solvent Polarity and Polarizability. *J. Phys. Chem. B* **2015**, *119* (2), 420−432.
(52) Kardas, T. M.; Ratajska-Gadomska, B.; Lapini, A.; Ragnoni, E.; Righini, R.; Di Donato, M.; Foggi, P.; Gadomski, W. Dynamics of the Time-Resolved Stimulated Raman Scattering Spectrum in Presence of Transient Vibronic Inversion of Population on the Example of Optically Excited Trans-β-Apo-8′-Carotenal. *J. Chem. Phys.* **2014**, *140* (20), 204312.
(53) Sovdat, T.; Bassolino, G.; Liebel, M.; Schnedermann, C.; Fletcher, S. P.; Kukura, P. Backbone Modification of Retinal Induces Protein-like Excited State Dynamics in Solution. *J. Am. Chem. Soc.* **2012**, *134* (20), 8318−8320.
(54) Demoulin, B.; Altavilla, S. F.; Rivalta, I.; Garavelli, M. Fine Tuning of Retinal Photoinduced Decay in Solution. *J. Phys. Chem. Lett.* **2017**, *8* (18), 4407−4412.

DOI: 10.1021/acs.jpca.7b10255
J. Phys. Chem. A 2018, 122, 955−964